OPEN ACCESS

GAVIN PUBLISHERS

Current Trends in Forest Research

Lawson SS, et al. Curr Trends Forest Res: CTFR-113.

Research Article

DOI: 10.29011/ CTFR-108. 100013

RNAseq Analysis of Figured and Non-Figured *Acacia koa* Wood

Shaneka S. Lawson[1*], Ketaki P. Bhide[2], Jyothi Thimmapuram[2]

[1]Department of Forestry and Natural Resources, USDA Forest Service, Purdue University, USA

[2]Department of Bioinformatics Core, Purdue University, USA

[*]**Corresponding author:** Shaneka S. Lawson, 715 W. State Street, USDA Forest Service, Northern Research Station, Hardwood Tree Improvement and Regeneration Center (HTIRC), Purdue University, PFEN126A, W. Lafayette, Indiana 47907, USA. Tel: +17658088188; Fax: +17654949461; Email: sslawson@fs.fed.us

Citation: Lawson SS, Bhide KP, Thimmapuram J (2018) RNAseq Analysis of Figured and Non-Figured *Acacia koa* Wood. Curr Trends Forest Res: CTFR-113. DOI: 10.29011/ CTFR-108. 100013

Received Date: 10 April, 2018; **Accepted Date:** 16 April, 2018; **Published Date:** 23 April, 2018

Abstract

Koa (*Acacia koa*) are tropical hardwoods endemic to the Hawaiian archipelago and a source of highly figured wood. Technological advancements, combined with our greater understanding of wood fiber development, allow us to use more in depth methods to study the figured wood phenomenon. This study represents the first transcriptomic analysis of figure formation in koa. Transcriptome profiles of figured and non-figured koa indicated that 19 genes were differentially expressed (DE) to a significant level (FDR < 0.05) between highly figured (HiFig), lightly figured (LoFig), and non-figured koa (NoFig) that were also involved in lignin biosynthesis, the phenylpropanoid pathway, jasmonate biosynthesis, and sucrose – starch synthesis. A total of 1,663 genes were identified where HiFig significantly differed from LoFig and NoFig at FDR < 0.05 and, at FDR < 0.01, the number was reduced to 958 candidate genes for further evaluation. Genes were further filtered at log2FC of +/- 2 in at least one pairwise comparison, resulting in a reduction from 1,663 and 958 to 341 and 221 genes. The direct role of any one transcript in generation of figure is not yet understood however, we note WAT1 and 5NG4 as candidates for future, more directed studies of the figured wood phenomenon.

Keywords: *Acacia koa*; Figured Wood; Lignin Biosynthesis; RNAseq; Transcriptomics

Introduction

Wood originating from a diverse array of tree species differs in form and strength. When comparisons are made between tree species, the most common explanations for the erraticism in strength were variation in abundance and orientation of the xylem polymers cellulose, hemicellulose, and lignin [1,2]. Disarray of xylem polymers, or spiraling, can be a common phenomenon in many tree species. While often a very visually appealing trait, spiraled wood is unsuitable for use in construction as the strength and stability of the material is compromised [3-5].

Koa (*Acacia koa*) is among more than twelve hundred members of the genus *Acacia* and is one of the most valuable tropical hardwoods in the world. Koa trees can grow to be nearly one 30 meters tall and more than nine meters in circumference. Koa trees also exhibit variability between both colour and figure. Figure is a variation or distortion of the natural grain patterning within a tree so that wood cell fibers no longer appear uniform in direction or alignment. Disparities in the alignment of wood cells can be identified as interlocked, irregular, spiral, or wavy [6]. Interlocked grain is the term used when spiraling wood periodically switches directionality from left to right [4]. This alternation in direction can provide additional stability and is more desired that a simple spiral pattern. Interlocked grain has been reported in a significant number of tropical tree species and may decrease risks associated with radial splitting in adult trees with spiral grain patterns [7].

Despite concentrated efforts by numerous researchers, we are still no closer to elucidating the mechanisms behind figure formation in any of the species that exhibit the trait. Recent findings have suggested figure development is not linked exclusively to genetics nor can environmental stressors be the main cause for its generation [8,9]. Throughout the 1900s the "birds-eye" variety of figure was proposed to be linked to numerous developmental mechanisms such as adventitious bud formation, abnormal

metabolic processes, and plant defense response to bird-peck injuries and insect damage [10,11].

Regardless of conjecture and anecdotal remarks regarding how figure is developed and how it may be propagated; no scientific evidence has been made available. However, figure can be generated in response to compression in the form of tension wood or formed during burl development. Burls are bark encased tumor-like growths that can be found on trunks, branches, or even on underground tissues. Grain patterns within burls are often abnormal, have been attributed to the existence of dormant buds, and can reliably be assumed to contain figure. Research has shown that crotch wood has also consistently exhibited figure. These three instances are the only known concessions to the theory that figure formation cannot be predicted. Few other theories have proven to be accurate in the prediction of figure establishment although the possibility exists that conventional breeding or grafting can be used to propagate figured individuals. Reliably produced figure is most likely the result of a combination of genetics and exposure to a particular set of environmental factors.

Wood formation is the result of an intricately coordinated and complex process that has yet to be fully understood. Numerous genes and gene families are involved in varied aspects of tree growth from programmed cell death and the formation of heartwood, to cell differentiation into bark and phloem. The phenylpropanoid pathway is extensive and connected to everything from production of anthocyanins and flavonoids, to generation of lignin and wood. A lengthy sequence of reactions is used to convert phenylalanine into many end products including lignin in plants **(**Figure S1**)**. Lignin is a complex polymer of monolignols and the final destination for nearly 30% of carbon fixed during photosynthesis. It is second to cellulose as the most abundant organic polymer in plants and on Earth [12,13]. The role of lignin is to provide rigidity for cell walls, protect cells from pathogens, and maintain osmotic potentials by preventing water intrusion. There are three possible forms of lignin resulting from the phenylpropanoid pathway H, R, and S. The primary forms found in softwoods are G, and to a lesser degree, H. Hardwoods are primarily composed of G and S lignin.

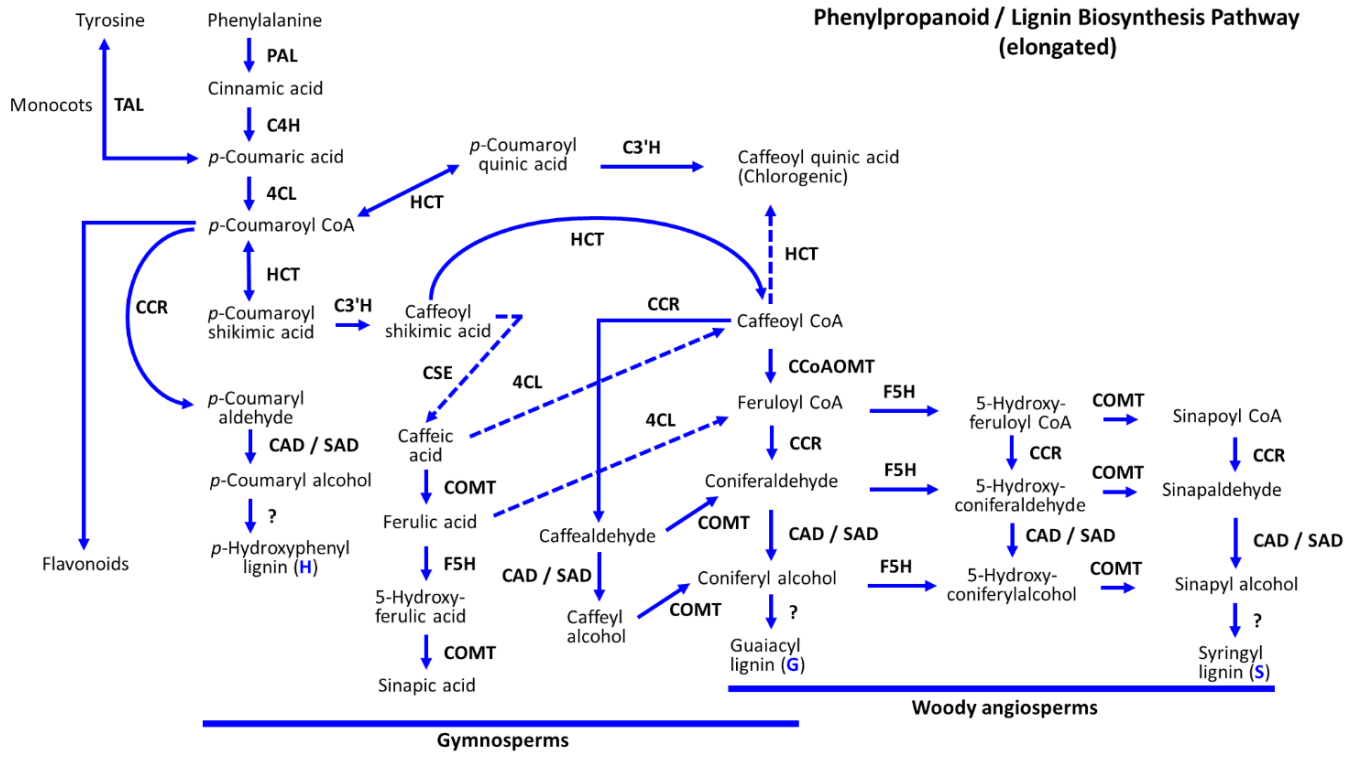

Figure S1: Rendering of more complete Phenylpropanoid and Lignin Biosynthesis Pathways unlike the simplified version depicted in the manuscript.

Sucrose metabolism requires cleavage of multiple isoforms of sucrose synthase by invertases to aid numerous biochemical processes within plants such as biosynthesis of cell wall components and cell expansion. Thus, enzymes responsible for cleaving sucrose are also instrumental in the regulation of cell wall development by influencing the regulation of cell wall differentiation genes

[14]. Methyl jasmonate is a volatile organic compound derived from jasmonates (JAs) which is produced in response to wounding and other biotic and abiotic stresses. This compound stimulates synthesis of defense chemicals [15], resin ducts [16], and has roles in cell death [17]. Additionally, JAs affect the signal stimulation and regulation of nodules in legumes [18]. The DE genes within these three pathways were selected for further study in figured and non-figured koa, as there exists many gaps in our knowledge of how genes in these pathways function for species outside of traditional model plant species.

This project used RNAseq combined with Illumina sequencing to characterize the upregulation or downregulation of genes that may be linked to the formation of figure. We used previously published pathway information for species such as *Arabidopsis* (*Arabidopsis thaliana*), soybean (*Glycine max)*, and poplar (*Poplar trichocarpa*) as the basis for incorporation of genes discovered during data analysis for koa. The tetraploid genome of koa is unusual as most trees species are diploid. However, exceptions have been found in some species of oak [19], poplar [20], and apple (*Malus* × domestica) [21]. This study benefits examinations of other tree species that form figure such as ash (*Fraxinus* spp.), walnut (*Juglans* spp.), maple (*Acer* spp.), and poplar (*Populus* spp.) by providing a selection of genes for the basis of initial figure analyses. We must stress that the figure examined here is from a section of the bole that displayed high, low, or no figure across our cookie sample. We do not make claims that our cookie sample is representative of the entire tree.

The pathways presented here may ultimately be adjusted as more information is obtained regarding regulation of the genes therein. It is not our intention to uncover every possible gene involved in the process rather, to narrow down the possibilities by a significant number so that additional studies on these particular genes can be implemented. We found thousands of differentially expressed (DE) genes but narrowed that number based on comparison of highly-figured (HiFig), low level figure (LoFig), and non-figured (NoFig) samples. We hypothesize that the genes identified in this study are indeed involved in the initiation and development of figure formation in koa.

Methods

Fourteen cookie samples (5 HiFig, 5 LoFig, and 4 NoFig) were taken from a private koa plantation undergoing harvest located on Hawai'i Island. As each tree was felled, a cookie was cut from the stump end, immediately placed into a pre-labeled bag, and buried in dry ice. The frozen cookies were packaged and shipped from Hawai'i to Purdue University in Indiana. The bags were removed from dry ice and placed into a -80 °C freezer immediately upon arrival at Purdue. A simple flow chart of the process (Figure S2).

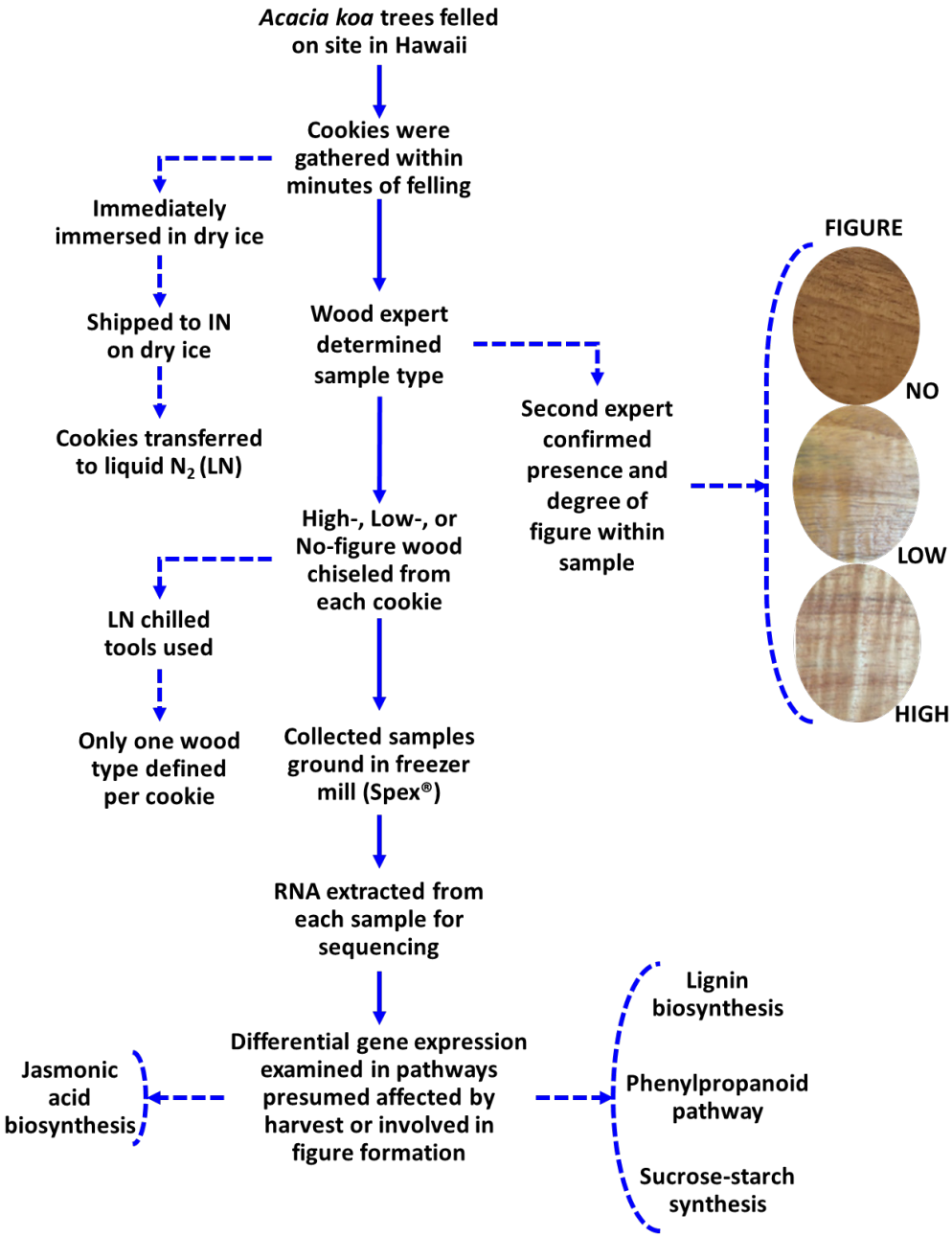

Figure S2: Experimental flow chart. Simplified version of experimental progression with examples of non-figured, lightly-figured, and highly-figured wood designations.

RNA Extraction

Cookies were cut into smaller chunks and categorized as high-, low-, or no-figure by two independent wood experts at the Purdue University Wood Research Lab (https://ag.purdue.edu/fnr/Pages/labwoodresearch.aspx). Cookies were removed from the freezer and placed in a steel pan of liquid nitrogen before being broken into slices with a pre-chilled hammer and chisel. The slices were then collected and placed into labeled 50 ml conical tubes (Corning®, USA) and moved to the -80 °C freezer. After resting for 24 h, individual tubes were removed, and the contents were placed into a freezer mill tube (SPEX®, USA) and presoaked in liquid nitrogen before the wood slices were ground into powder. The freshly ground powder was again placed in the -80 °C freezer overnight. RNA was extracted from the wood using the RNeasy® Plant Mini Kit (QIAGEN®, Germany) the following day. Resultant RNA yield was examined by Nanodrop 8000 (Thermo Fisher Scientific Inc., USA) after the addition of 1 µl RNasin® (Promega Corporation, USA). RNA quality was determined on an RNA 6000 nano chip (Agilent Technologies, USA) after denaturation and final quality confirmed with an electropherogram.

RNA Library Construction

Fourteen barcoded libraries were generated according to manufacturer's instructions for the Illumina RNA TruSeq kit (Illumina®, USA). A total of 2 µg of high quality RNA was used for each individual sample. Library quality was determined using the Agilent Bioanalyzer 2100 (Agilent Technologies, USA) before the barcoded libraries were pooled to ensure equimolar sample representation. The libraries were reverse-transcribed and sequenced on the Illumina HiSeq2000 platform. *De novo* assembly using Transcriptome Assembly by Short Sequences (Trans-ABySS, v.1.5.3) was employed to generate a reference transcriptome.

De Novo Assembly and Annotation

De novo transcriptome assembly using Trinity (v.3.0) was performed on the short RNA sequences to generate a reference transcriptome containing reference contigs. Contigs ≥ 500 bp were filtered and used for downstream analysis and annotation based on BLASTX against the non-redundant (nr) protein database from NCBI (http://blast.ncbi.nlm.nih.gov/), and the poplar and soybean (Glycine max) protein databases from Phytozome (v.10; https://phytozome.jgi.doe.gov/). Contigs with blast hits in any of the selected databases and E-values less than 10^{-3} were considered annotated. The longest putative coding sequences (ORFs) were predicted from contigs using the Trinity transdecoder utility at default parameters (except 'stranded' parameter). ORFs with the highest scores were selected using the Markov model (log likelihood ratio based on coding/non coding) in each of the six reading frames possible. Predicted ORFs were searched against the Pfam database to also obtain predicted peptides for contigs. Full-length transcripts were identified using BLASTX against the Swissprot database. Transcripts with greater than 80 percent alignment coverage to Swissprot hits were retained as full length.

Read Quality and Mapping

FastQC (v.0.11.2) and the FASTX toolkit (v.0.013.2) were used to assess the quality of each sample sequence and to execute quality trimming. Bases with Pfred33 scores below 30 were removed. Reads with greater than 50 bases (99% of total reads) were kept for further downstream analysis. Bowtie2 (v.2.2.6) was used to map quality trimmed reads against the *de novo* assembled transcriptome for koa using default parameters.

Transcript Abundance and Differential Expression

The RSEM tool within Trinity was used to estimate transcript abundance. Transcript length, number of reads mapped to transcript, and total number of reads were taken into account. The RSEM-EBSeq tool was employed to find differentially expressed (DE) contigs between two groups (HiFig vs LoFig, HiFig vs NoFig, LoFig vs NoFig) and across multiple groups (HiFig, LoFig, NoFig) at PPDE ≥ 0.95 (FDR ≤ 0.05). Specific expression patterns (Patterns 2 and 4) were identified and selected from expression across all three groups using RSEM-EBSeq **(**Table 1**)**. When multiple DE contigs were annotated to same soybean protein the average of logFC values were used for pathway characterization and EBSeq pattern assignments. Expected counts generated from RSEM-EBSeq were used as input for DESeq2 (v.1.8.1). In DESeq2, distribution counts for the two experimental conditions were tested to identify DE genes with p-values and adjusted p-values of false discovery rate (FDR) to correct for multiple tests by DESeq2.

Pattern	HiFig	LoFig	NoFig	Transcripts
1	A	A	A	67,934
2	A	A	B	34
3	A	B	A	6,775
4	A	B	B	8,785
5	A	B	C	3

Table 1: Pattern identification. Significant differences in transcript gene expression across comparative samples.

Pathway Analysis of DEGs

Contigs annotated using BLAST were then allocated to four pathways of interest; Phenylpropanoid, Lignin Biosynthesis, Jasmonic acid Biosynthesis, or Sucrose-Starch synthesis using MapMan (v.3.6.0). MapMan (Mercator pipeline) was used to generate pathway 'bins' and preliminary figures using soybean protein sequences as no annotation is available for koa genes. Information regarding the roles of the annotated genes was obtained from NCBI (http://www.ncbi.nlm.nih.gov/gene) and manuscripts

published in Web of Science (http://apps.webofknowledge.com/). Heatmaps of these annotated genes were also generated for 'Pattern 2' and 'Pattern 4' genes using HeatmapGenerator5_MacOSX (https://sourceforge.net/projects/heatmapgenerator/).

Results

Analysis of Mapped Read Quality

Freshly sawn cookies from five HiFig, four LoFig, and five NoFig individuals of the tetraploid tree species koa were subjected to RNASeq analysis. Each HiFig sample averaged approximately 31.87 million 100 bp reads with numbers for LoFig and NoFig koa samples averaging 31.85 million and 27.13 million reads. All samples had about 98-99% of reads passing quality control with an average mapping rate of about 61% (Table 2).

	Ttl. Reads (Avg)	Quality Reads (Avg)	% Passing QC (Avg)	Total Mapped (Pairwise Avg)	Mapping Rate (Avg)
HiFig	31,873,475	31,670,910	99.37	38,999,838	61.98
LoFig	31,853,051	31,609,266	99.24	37,801,811	60.45
NoFig	27,127,237	26,932,403	99.28	32,778,058	60.82
Overall Avg	**30,284,588**	**30,070,860**	**99.30**	**36,526,569**	**61.08**

Table 2: Mapping statistics. Number of reads mapping back to the *de novo* koa transcriptome.

Contigs and Alignments

A total of 683,388 contigs ≥ 500 bp were generated by Trinity for downstream analysis. The longest contig assembled was 20,448 bp. There were 33 contigs greater than 10,000 bp and 1,636 greater than 5,000 bp. Predicted protein and mRNA sequences were obtained for 119,932 of 683,388 contigs (Table 3). Contigs with greater than 80% alignment in the Swissprot database were retained, resulting in 14,154 contigs. There were 292,418 contigs with hits to the nr database representing 47.8% of contigs with database hits. Additionally, 275,009 (40.2%) had hits to the soybean protein database, 254,937 (37.3%) had hits to the poplar database, and 244,208 (35.7%) had hits to all 3 databases.

Category	Large Contigs	All Contigs
Min. contig size	500	n/a
No. of contigs	683,388	2,019,460
No. of bases	730,029,444	1,131,682,574
Contig size range	500 – 20,488	0 – 20,488
N50	1,171	729
# sequences at N50+	189,650	n/a
Average length	1,068	560

Table 3: Contig data. Breakdown of contig information from transcriptome analysis.

Further narrowing of these contigs by pattern identification resulted in 20,380 transcripts that were greater than 90% identical to a gene within the database. Increasing stringency yielded 6,664 unique transcripts greater than 95% identical and 1,050 transcripts with 100% identity (Table 4). When evaluating the soybean database exclusively there were 1,116 100% identical matches and 1,481 95% identical matches to individual gene transcripts.

		HiFig vs LoFig	HiFig vs NoFig	LoFig vs NoFig
DESeq2				
p-value	$p < 0.05$	38,763	19,739	21,060
	$p < 0.01$	9,105	3,987	4,246
	$p < 0.001$	1,306	704	496
p-value (Adj)	$p < 0.05$	290	176	0
	$p < 0.01$	48	76	0
	$p < 0.001$	4	29	0
RSEM-EBSeq				
	FDR < 0.05	6,057	906	288

Table 4: Stringency counts. Unique differentially expressed transcripts identified by both DESeq2 and RSEM-EBSeq methods.

Gene Expression Profiles

Total mapped reads for all transcripts were used in analysis of the variation in gene expression between HiFig, LoFig, and NoFig samples. A total of 290 genes were either up or downregulated between HiFig and LoFig samples and only 176 genes between HiFig and NoFig using DESeq2. Analysis with RSEM-EBSeq

indicated 6,057 genes DE between HiFig and LoFig compared to 906 genes for HiFig and NoFig. An overlap of 174 genes were identified from HiFig versus LoFig genes and 127 genes from HiFig versus NoFig using both RSEM-EBSeq and DESeq2 (Figure 1). Of the 290 genes identified using DESeq2, 213 were downregulated and 21 were upregulated for HiFig to LoFig compared to upregulation of 383 genes and downregulation of 967 genes from the 6,057 DE genes identified. The HiFig to NoFig comparison resulted in 176 DE genes with upregulation of only 2 genes and the downregulation of 51 genes using DESeq2. Use of RSEM-EBSeq resulted in 906 DE genes with 16 genes upregulated and 359 genes downregulated. There were no DE genes identified using DESeq2 for the LoFig to NoFig comparison. However, 288 DE genes were isolated using RSEM-EBSeq. There were 47 upregulated genes and 32 downregulated genes identified (Table 5). Use of both DESeq2 and RSEM-EBSeq methods generated consistent results.

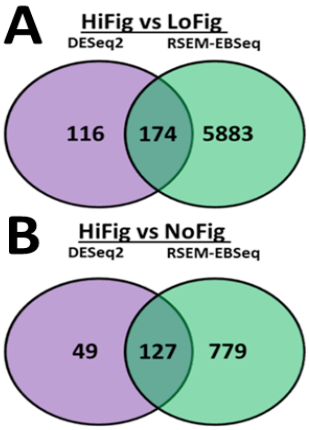

Figure 1: Venn diagrams. **(a)** Illustration of the number of genes differentially expressed in HiFig versus LoFig and **(b)** HiFig versus NoFig individuals.

Name	Locus ID	Change in Expression (log2FC)			Change in Expression (Mean)		
		Hi vs Lo	Hi vs No	Lo vs No	HiFig	LoFig	NoFig
Pattern 2							
Uncharacterized	Glyma.03G099600.1	0.029153127	-1.01428975	-1.043442877	3.282475356	3.253322229	4.296765106
5NG4	Glyma.04G250900.1	-0.580251734	2.430746071	3.010997805	5.124257831	5.704509565	2.69351176
Unknown	Glyma.05G125800.1	-0.102524937	2.283929111	2.386454048	5.45626926	5.558794197	3.172340149
Unknown	Glyma.05G183500.1	-0.134967819	-3.035027064	-2.900059245	2.065220018	2.200187837	5.100247082
P21	Glyma.05G204800.1	-0.590941495	-3.443346778	-2.852405283	3.901037988	4.491702718	7.340506732
Unknown	Glyma.06G084200.1	-0.034364364	3.538202697	3.572567061	5.063288402	5.09192193	1.550856192
TPR	Glyma.07G127400.1	0.363261743	1.813331501	1.450069758	3.978316456	3.615054713	2.164984955
WAT1	Glyma.08G182500.5	-0.303444199	2.505224963	2.808669163	6.728099369	7.152873516	4.134732222
Uncharacterized	Glyma.11G119200.1	0.600719236	3.065765126	2.46504589	7.15462924	6.553910005	4.088864114
PRA1.H	Glyma.13G273800.1	0.078768676	1.005390031	0.926621355	5.15614126	5.077372584	4.150751229
WAT1	Glyma.14G148100.1	-0.063761829	2.520716332	2.584478162	7.018743897	7.01936246	4.501619795
WAT1	Glyma.15G049800.1	0.00784575	2.782509056	2.774663306	7.892388845	7.884543096	5.10987979
Unknown	Glyma.15G049900.1	0.136527351	2.548701126	2.412173775	5.019293847	4.882766497	2.470592721
Uncharacterized	Glyma.15G086800.1	-0.038691016	-2.880348615	-2.841657599	2.489596554	2.538918075	5.389394159
PM ATPase	Glyma.17G061800.1	-0.18393989	2.379815477	2.563755367	4.144699213	4.328639103	1.764883736
CYP71A20	Glyma.17G125400.1	-0.040455609	3.202722739	3.243178347	4.925354917	4.965810526	1.722632178
AAT1	Glyma.20G036300.1	-0.668306739	2.48159134	3.149898079	5.622676675	6.279759431	3.185096086
Phenylpropanoid Pathway							
DFR	Glyma.01G017100.1	-0.554556369	-0.331751422	0.222804947	5.277401253	5.831957622	5.609152675
KYAT1	Glyma.02G014800.1	-1.070486705	-0.977536349	0.092950356	3.137339713	4.380360268	4.178584552
HCBT1	Glyma.02G185100.1	-0.14945244	0.622464299	0.771916739	6.687943081	6.83739552	6.065478782
BAHDAT	Glyma.03G078200.1	0.061025626	-0.042615279	-0.103640906	4.258307245	4.782364645	4.426520317
Uncharacterized	Glyma.04G039900.1	1.220710968	0.619920765	-0.600790203	4.10377592	2.883064952	3.483855155

Uncharacterized	Glyma.04G251800.1	-0.498951462	0.044518866	0.543470328	5.556812161	6.316276236	5.858873811
Uncharacterized	Glyma.05G092400.1	-1.713909586	-1.169501097	0.544408489	3.54091632	5.675296836	4.40584563
MAT	Glyma.06G111000.1	0.059076343	0.074298674	0.01522233	4.551480462	4.844223442	4.771453283
ROMT	Glyma.06G286200.1	1.268291811	0.74280333	-0.525488481	3.538081466	2.269789655	2.795278136
ROMT	Glyma.06G286600.1	-0.491558224	0.276378627	0.767936851	4.211718861	4.894329211	3.828839579
CCR	Glyma.07G026300.1	-1.471433739	-1.0834021	0.388031639	4.010873308	5.450621542	5.17902804
LAC7	Glyma.07G142400.1	0.724317198	0.259958557	-0.464358641	4.430691626	3.706374428	4.170733069
NIC1	Glyma.08G067600.1	-0.902155894	-0.548553141	0.353602753	6.209349132	7.097117198	6.696229146
NIC1	Glyma.08G279200.1	-0.138599873	-0.109645245	0.028954628	3.669145315	3.979009647	3.749940452
CCR2	Glyma.09G205700.1	-0.488689767	-0.327239478	0.161450288	7.272006287	7.760696053	7.599245765
TKPR2	Glyma.09G205700.2	-0.615374676	-0.126309767	0.489064909	3.330611496	3.945986173	3.456921263
IFR	Glyma.09G211500.1	-1.525926321	0.354925038	1.880851359	7.234641281	8.761355087	6.914093645
IFR	Glyma.09G211500.2	-1.175825107	-0.078727932	1.097097175	3.175213766	4.431092366	3.15359057
IFR	Glyma.09G211600.1	-0.816334601	1.229841359	2.04617596	4.63449792	5.49707164	3.409942716
NUC2	Glyma.09G283200.1	-0.073624437	-0.092418186	-0.018793749	5.829242046	6.581952776	6.290567127
IF7OMT6	Glyma.10G176500.1	1.605960717	1.223189502	-0.382771215	3.61424062	2.008279903	2.391051118
HHT1	Glyma.11G231600.1	0.88656568	0.369023717	-0.517541963	4.099125328	3.382199253	3.847652481
DBAT	Glyma.13G232400.1	0.180454421	0.912080372	0.731625951	4.678626079	4.565320823	3.770771484
SHT	Glyma.14G031100.1	1.00279276	1.080602754	0.077809994	4.064849447	3.139360126	2.964878279
HHT1	Glyma.14G057700.1	-0.802239727	-1.19158522	-0.389345493	5.285514715	6.085146245	6.475601066
FBT6	Glyma.14G101100.1	-0.480984551	-0.177980358	0.303004194	3.568025798	4.122801684	3.748982789
HHT1	Glyma.14G110500.1	2.01318471	0.701995808	-1.311188902	3.697826763	1.684642053	2.995830955
ROMT	Glyma.14G201100.1	1.151162158	0.4777048	-0.673457358	4.140287452	2.921211517	3.588467612
OPCL1/4CL5L	Glyma.14G223200.1	-1.118951831	-0.723824852	0.395126978	7.249021596	8.367973427	7.972846449
CCR2	Glyma.15G125100.1	-0.397390584	-0.159468017	0.237922568	5.596386354	6.061539355	5.830936623
SHT	Glyma.16G039500.1	-0.047232864	0.16243061	0.209663474	3.653352149	3.746454717	3.573121797
IFR	Glyma.16G103900.1	-0.648305851	-0.79036686	-0.142061009	5.60070908	6.249014931	6.39107594
SHT	Glyma.17G061000.1	1.473796744	0.720800563	-0.752996181	3.762427017	2.288630273	3.041626454
Uncharacterized	Glyma.17G152600.1	0.475941598	0.514022952	0.038081355	3.687847989	3.258946466	3.20054486
I4OMT	Glyma.18G269600.1	-0.002759121	0.017232456	0.019991577	5.458080726	5.460839847	5.44084827
4CLL9	Glyma.19G075800.1	0.426845684	0.036316605	-0.390529079	3.334460323	2.907614638	3.298143717
OPCL1/4CL5L	Glyma.20G192100.1	-0.213251796	0.930798286	1.144050082	5.734364615	5.930015139	4.808565734
Lignin Biosynthesis							
CCR	Glyma.02G230500.1	-1.650005195	-1.230768311	0.419236883	2.104359456	3.754364651	3.335127768
CCR	Glyma.02G230500.2	-2.00219169	-1.520739697	0.481451994	3.344750462	5.346942153	4.865490159
CYP71B34	Glyma.07G160700.3	1.653091045	1.478292463	-0.174798581	3.979600701	2.326509656	2.501308238
SAM_DM	Glyma.08G175700.2	1.247911041	1.010930226	-0.236980816	3.996820817	2.748909776	2.985890591
CCR	Glyma.11G164700.1	-2.472865425	-2.295406885	0.177458539	2.718658475	5.191523899	5.01406536
CCR	Glyma.14G197600.3	-1.705343706	-1.325317663	0.380026043	3.156719244	4.86206295	4.482036907

Jasmonate Acid Biosynthesis							
TIFY-6A / JAI3	Glyma.05G235500.5	-1.241169211	-1.09612794	0.145041271	7.966635005	9.207804216	9.062762945
TIFY-6B / JAI3	Glyma.08G043000.2	-1.198420877	-1.018358769	0.180062108	6.581517398	7.779938274	7.599876167
LOX10	Glyma.08G189600.1	2.101127699	1.014404829	-1.086722869	4.551603324	2.450475626	3.537198495
LOX2.1	Glyma.13G075900.1	-2.916104731	0.217172031	3.133276762	3.52446249	6.440567221	3.307290459
Sucrose – Starch Synthase Pathway							
FLN2	Glyma.01G062100.1	-1.361517101	0.375128036	1.736645137	2.589073676	3.950590777	2.21394564
Sus7	Glyma.02G240400.1	-1.90866193	-1.936607402	-0.027945471	2.429141288	4.248619805	4.283271047
Sus2	Glyma.03G216300.1	-1.895033332	-1.813223263	0.081810069	8.243479731	10.13851306	10.05670299
SS4	Glyma.05G127800.1	2.262340512	0.650877237	-1.611463275	4.514216413	2.259203138	3.834696415
SPP1	Glyma.10G086600.2	-1.313767296	-1.162566618	0.151200679	5.657000561	6.955435021	6.799120909
FK5	Glyma.10G176900.1	2.016634614	0.356189759	-1.660444855	4.109855506	2.093220893	3.753665747
Sus7	Glyma.16G217200.1	-1.986106956	-1.913530771	0.072576186	3.214596727	5.20094454	5.146691418
Sus2	Glyma.19G212800.1	-2.037807731	-2.096327112	-0.058519381	9.178517416	11.21632515	11.27484453

4CLL9, 4-coumarate-CoA ligase-like 9; 5NG4, Auxin-induced transmembrane protein similar to Walls Are Thin1; AAT1, Vacuolar amino acid transporter 1; BAHDAT, BAHD acyltransferase; CCR, Cinnamoyl-CoA reductase 1; CCR2, Cinnamoyl-CoA reductase 2; CYP71A20, Cytochrome P450 family 71-subfamily A polypeptide 20; CYP71B34 "Cytochrome P450 family 71-subfamily B polypeptide 34; DBAT, 10-deacetylbaccatin III 10-O-acetyltransferase; DFR, Dihydroflavonol-4-reductase; FBT6, Probable folate-biopterin transporter 6; FK5, Probable fructokinase-5; FLN2, Fructokinase-like 2; HCBT1, Anthranilate N-benzoyltransferase protein 1-like; HHT1, Omega-hydroxypalmitate O-feruloyl transferase; I4OMT, Isoflavone 4'-O-methyltransferase; IF7OMT6, Isoflavone-7-O-methyltransferase 6; IFR, Isoflavone reductase; JAI3 / TIFY-6A, Jasmonate-zim-domain protein 3; JAI3 / TIFY-6B, Jasmonate-zim-domain protein 3; KYAT1, Kynurenine--oxoglutarate transaminase 1; LAC7, Laccase 7; LOX10, Linoleate 9S-lipoxygenase 10; LOX2.1, Linoleate 13S-lipoxygenase 2-1, chloroplastic; MAT, Methionine aminotransferase; NIC1, Nicotinamidase 1-like; NIC2, Nicotinamidase 2-like; OPCL1 / 4CL5L, 3-oxo-2-(2'-[Z]-pentenyl)cyclopentane-1-octanoate CoA ligase / 4-coumarate--CoA ligase-like 5; P21, P21-like protein; PM ATPase, Plasma membrane ATPase;PRA1.H, PRA1 family protein H; ROMT, Trans-resveratrol di-O-methyltransferase; SAM_DM, S-adenosyl-L-methionine-dependent methyltransferases superfamily protein; SHT, Shikimate O-hydroxycinnamoyltransferase; SPP1, Sucrose-6F-phosphate phosphohydrolase family pnrotein; SS4, Starch synthase 4; Sus2, Sucrose synthase 2; Sus7, Sucrose synthase 7; TKPR2, Tetraketide alpha-pyrone reductase 2; TPR, Tetratricopeptide repeat (TPR)-like superfamily protein; WAT1, Walls Are Thin1.

Table 5: Summary of genes highlighted in this study and their respective expression changes.

One of the primary objectives of this study was to compare genes expressed in koa trees with and without figure. A total of 1,663 genes were revealed that exhibited EBSeq Pattern 4. Where HiFig was significantly different from both LoFig and NoFig at FDR < 0.05 and, at FDR < 0.01, the number was reduced to 958 candidate genes for evaluation. Genes were further filtered at log2FC of +/- 2 in at least one pairwise comparison, hence numbers were reduced to 341 and 221 genes from 1,663 and 958 genes (Figure 2A, Figure 2B).

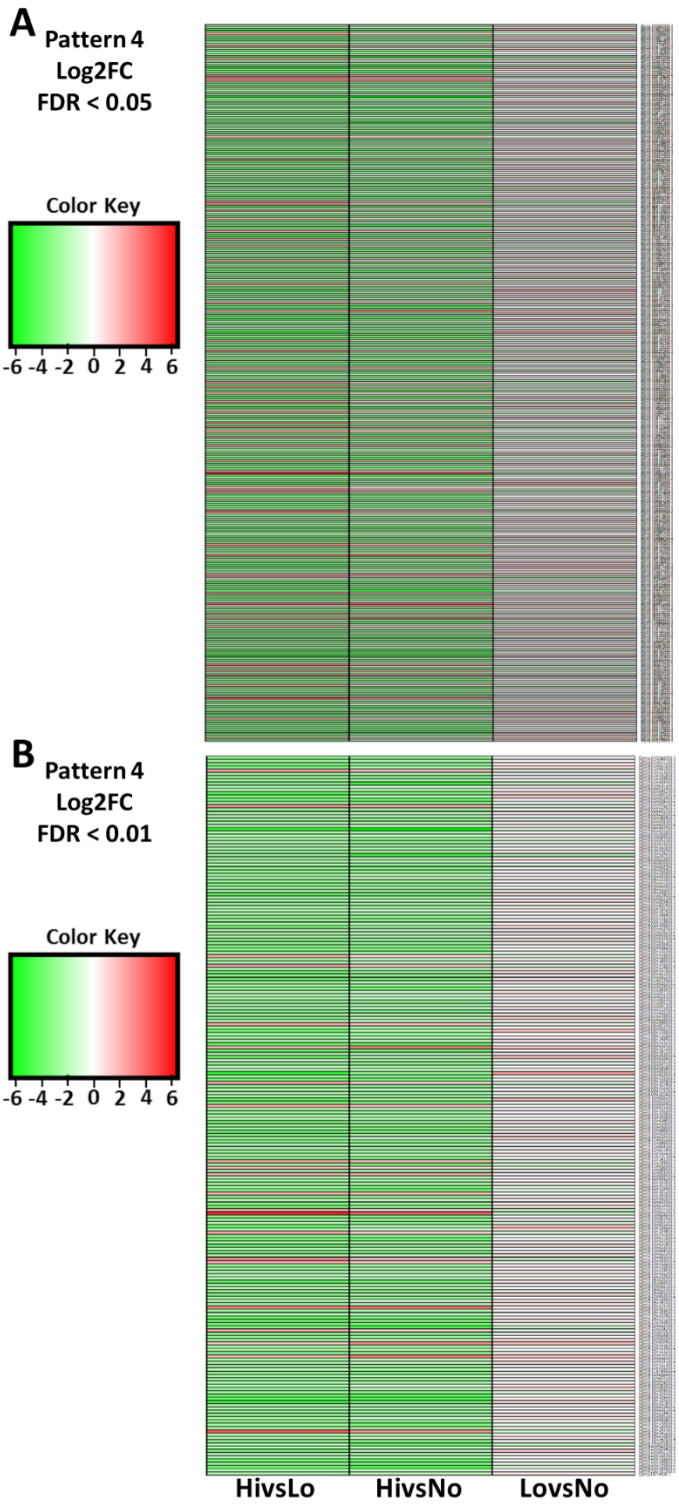

Figures 2(A-B): Heatmaps of 'Pattern 4' gene expression. **(A)** Pattern 4 genes isolated at a Log2FC and a FDR < 0.05 and **(B)** at FDR < 0.01. Upregulated (green, -2). Downregulated (red, 2).

We evaluated the number of genes that exhibited Pattern 2, when HiFig and LoFig significantly differed from NoFig. Seventeen genes were isolated using Log2Means (Figure 3A). After incorporation of Log2FC FDR < 0.1, 17 of these genes remained for further study (Figure 3B). Of these genes, four were unknown genes (Glyma.05G183500.1, Glyma.05G204800.1, Glyma.06G84200.1, Glyma.15G049900.1), three uncharacterized loci LOC100786119, LOC100306585, LOC100795405 (Glyma.03G099600.1, Glyma.11G119200.1, Glyma.15G086800.1), three WAT1-related proteins (2- At1g68170-like, 1- At4g08290-like) (Glyma.08G182500.5, Glyma.14G148100.1, Glyma.15G049800.1), an auxin-induced protein 5NG4-like (Glyma.04G250900.1), a tetrahydrocannabinolic acid synthase-like (Glyma.05G125800.1), a pentatricopeptide repeat-containing protein At3g14330-like (Glyma.07G127400.1), a PRA1 family protein H (Glyma.13G273800.1), a 12-oxophytodienoate reductase 3-like (Glyma.17G049900.1), a cytochrome P450 71A1-like (Glyma.17G125400.1), and a single vacuolar amino acid transporter 1-like (Glyma.20G036300.1).

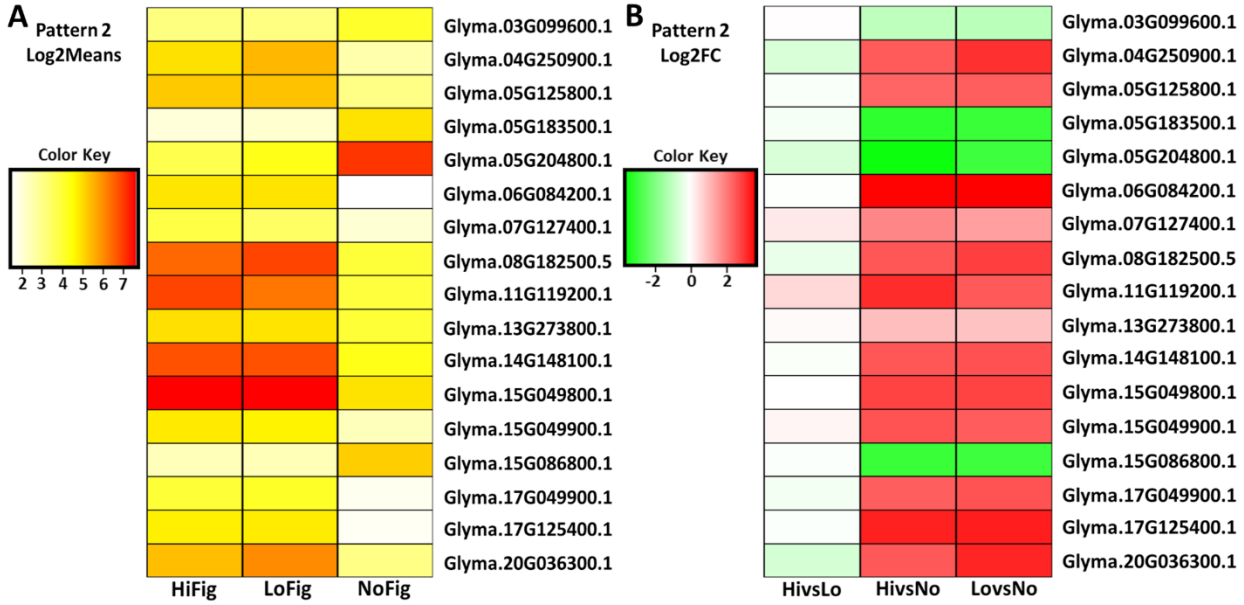

Figures 3(A-B): Heatmaps of 'Pattern 2' gene expression. **(A)** Pattern 2 genes isolated using Log2Means and **(B)** Log2FC. Upregulated (green, -2). Downregulated (red, 2).

Biosynthesis Pathway Analysis

In addition to genes described exhibiting the above patterns, the differentially expressed genes from four pathways involved in processes typically associated with wood formation were examined. DE genes involved in the phenylpropanoid (PP), jasmonic acid (JA), lignin biosynthesis (LB) and the sucrose – starch biosynthesis (SS) pathways were identified.

Phenylpropanoid Pathway Analysis

Genes that were DE to a significant degree within the PP pathway were visualized in two formats, Log2Means (Figure 4A) and Log2FoldChange (Figure 4B). This close examination of the PP resulted in the identification of 37 gene transcripts. Several dramatically different expression patterns were displayed among the three groups (HiFig, LoFig, and NoFig). Seven of the most pronounced differences between figured and non-figured samples were observed in those transcripts coding for trans-resveratrol di-O-methyl transferase-like (Glyma.06G286200.1, Glyma.14G201100.1), isoflavone reductase homolog (Glyma.09G211500.2), spermidine hydroxycinnamoyl transferase-like (Glyma.17G061000.1), omega-hydroxypalmitate O-feruloyl transferase-like (Glyma.14G110500.1), isoflavone-7-O-methyltransferase 9-like (Glyma.10G176500.1), and an uncharacterized acetyltransferase At3g50280 gene (Glyma.04G039900.1).

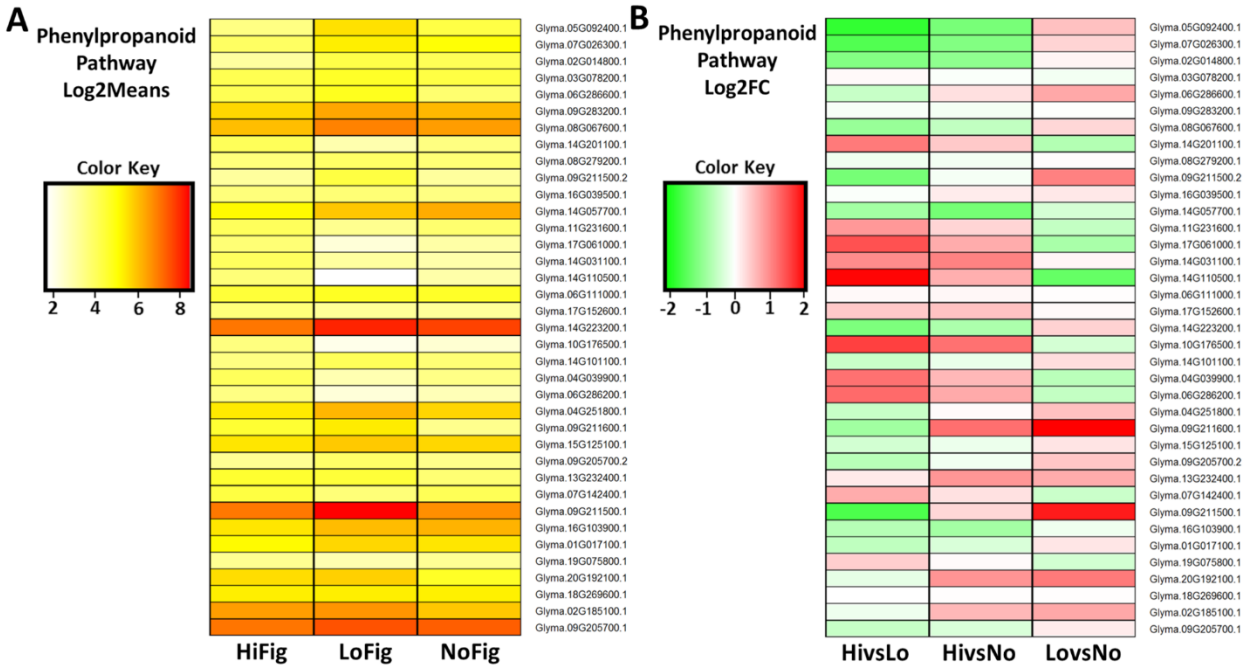

Figures 4(A-B): Heatmaps of Phenylpropanoid Pathway gene expression. **(A)** Phenylpropanoid Pathway genes isolated using Log2Means and **(B)** Log2FC. Upregulated (green, -2). Downregulated (red, 2).

Lignin Biosynthesis Pathway Analysis

There were numerous differentially expressed gene transcripts within the LB pathway. In addition to visualization of the Log2Means **(**Figure 5A**)** and Log2FoldChange **(**Figure 5B**)**, an additional stringency was applied. Use of FDR < 0.05 minimized the list of highly significant DE genes from 64 to the six most DE genes. The highlighted transcripts corresponded to four cinnamoyl-CoA reductase 1 genes (Glyma.02G230500.2, Glyma.14G197600.3, Glyma.02G230500.1, and Glyma.11G164700.1), a cytochrome P450 71D11-like gene (Glyma.07G160700.3), and a single O-methyltransferase MdmC-like gene (Glyma.08G175700.2) **(**Figure 5C, Figure 5D**)**.

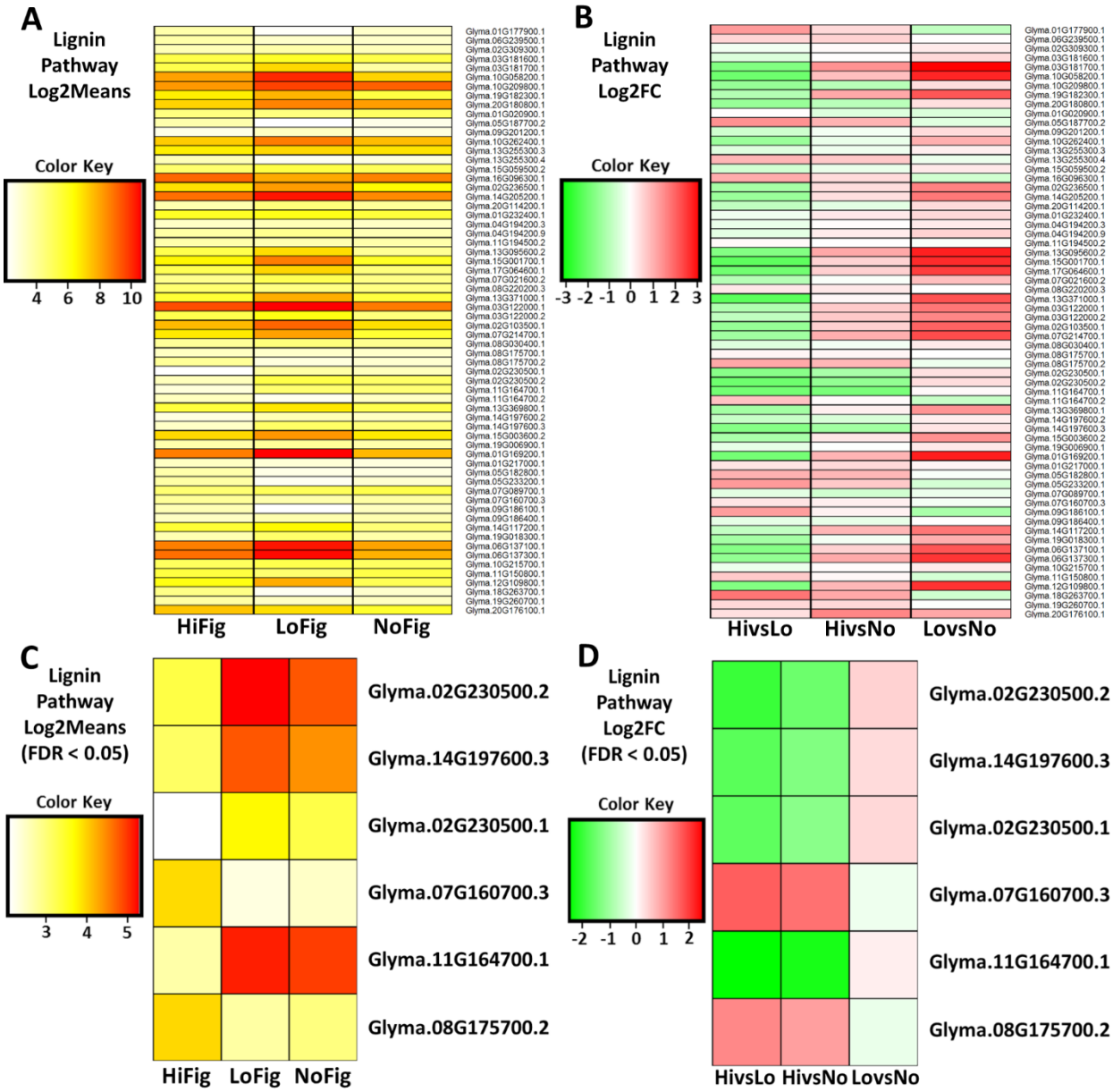

Figures 5(A-D): Heatmaps of Lignin Biosynthesis Pathway gene expression. **(A)** Lignin Pathway genes isolated using Log2Means, **(B)** Log2FC, **(C)** Log2Means with a FDR < 0.05, and **(D)** Log2FC with a FDR < 0.05. (**A**,**C**) Lower (yellow, 3), Higher (red, 10); (**B**,**D**) Upregulated (green, -2), Downregulated (red, 2).

Jasmonic Acid Biosynthesis Pathway Analysis

Analysis of the DE levels for genes assigned to the JA pathway revealed 45 gene transcripts of interest. These 45 transcripts were revealed after calculation of the Log2Means (Figure 6A) and Log2FoldChange (Figure 6B), however, only four transcripts remained after increasing the stringency to included FDR < 0.05. These four transcripts coded for TIFY 6A-like (Glyma.05G235500.5), TIFY 6B-like (Glyma.08G043000.2), linoleate 13S-lipoxygenase 2-1, chloroplastic-like (Glyma.13G075900.1), and lipoxygenase-10 (Glyma.08G189600.1) (Figure 6C, Figure 6D).

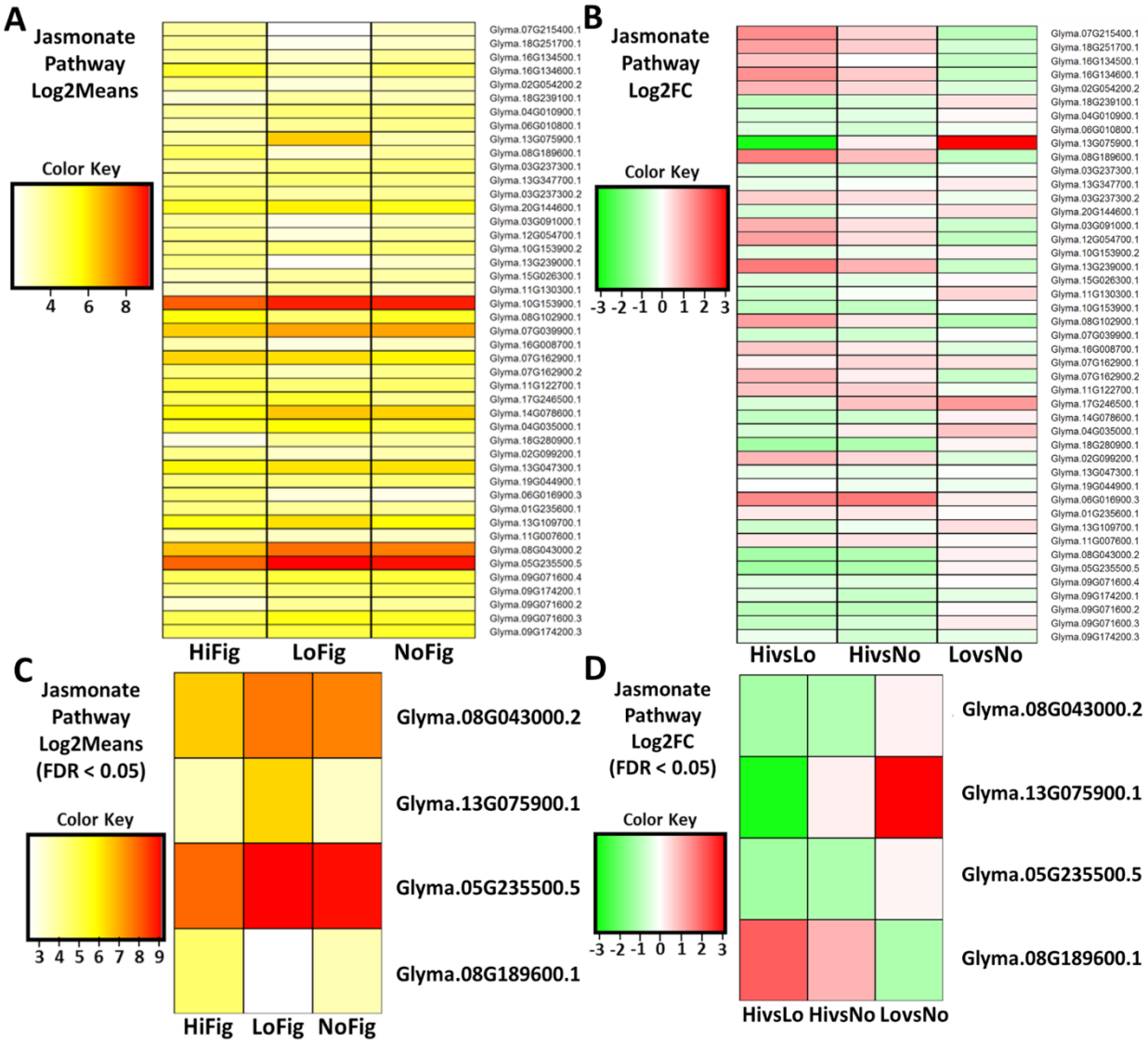

Figures 6(A-D): Heatmaps of Jasmonate Biosynthesis Pathway gene expression. **(A)** Jasmonate Pathway genes isolated using Log2Means, **(B)** Log2FC, **(C)** Log2Means with a FDR < 0.05, and **(D)** Log2FC with a FDR < 0.05. (**A**,**C**) Lower (yellow, 3), Higher (red, 9); (**B**,**D**) Upregulated (green, -2), Downregulated (red, 2).

Sucrose – Starch Synthesis Pathway Analysis

Examination of the DE genes in the SS pathway revealed the largest number of DE genes. There were 73 DE genes of interest identified in the sucrose-starch synthesis pathway after Log2Means (Figure 7a) and Log2FoldChange (Figure 7B) were applied to the raw data. The stringency was increased using FDR < 0.05 and 65 genes were eliminated. The remaining eight genes coded for two sucrose synthase 7-like genes (Glyma.02G240400.1, Glyma.16G217200.1), two sucrose synthase 2 genes (Glyma.03G216300.1, Glyma.19G212800.1), a probable starch synthase 4, chloroplastic/amyloplastic gene (Glyma.05G127800.1), a sucrose-phosphatase 1 gene (Glyma.10G086600.2), a fructokinase-like 2 (Glyma.01G062100.1), a single probable fructokinase-5 gene (Glyma.10G176900.1) (Figure 7C, Figure 7D).

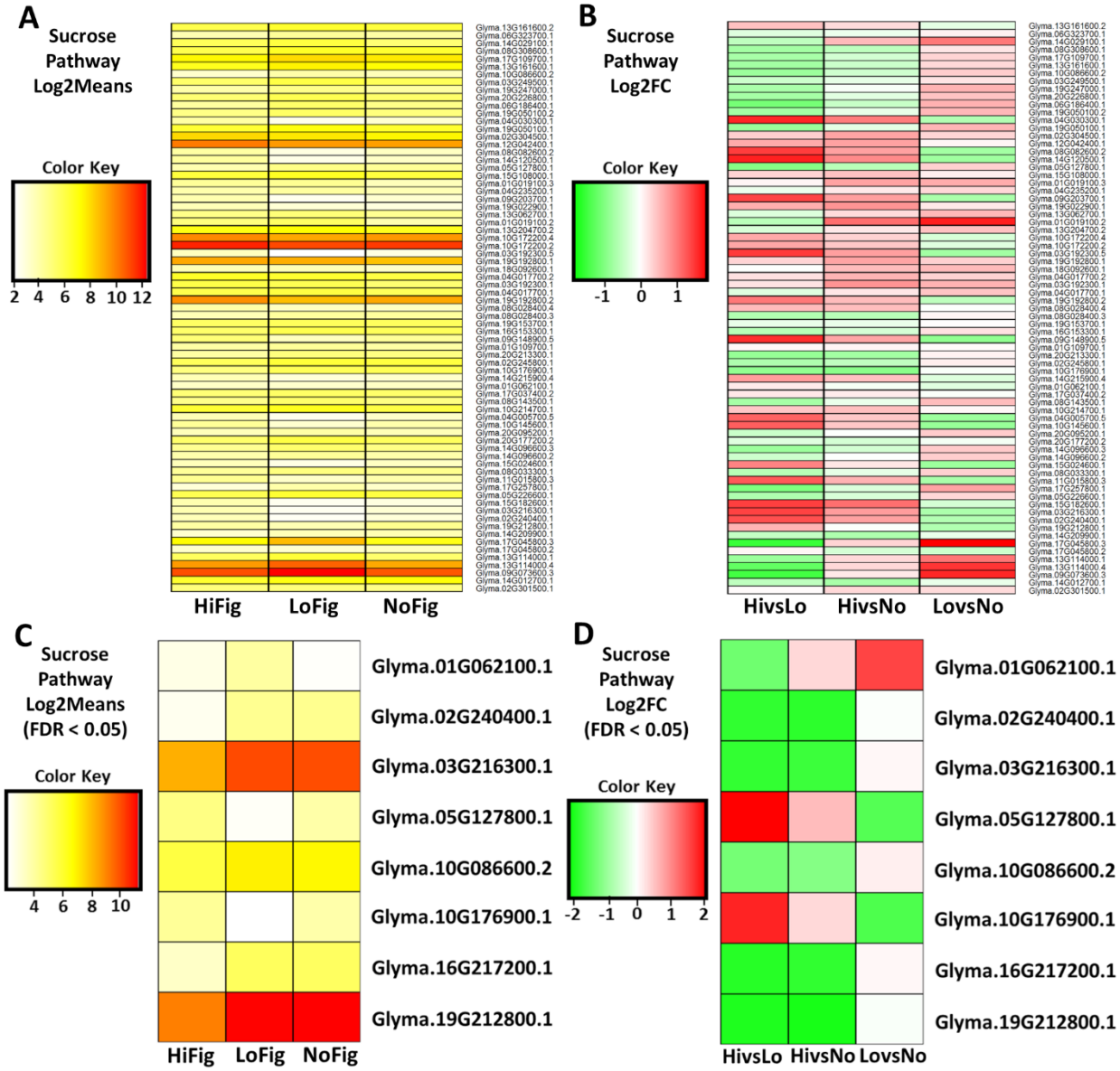

Figures 7(A-D): Heatmaps of Sucrose-Starch Biosynthesis Pathway gene expression. **(A)** Sucrose Pathway genes isolated using Log2Means, **(B)** Log2FC, **(C)** Log2Means with a FDR < 0.05, and **(D)** Log2FC with a FDR < 0.05. (**A**,**C**) Lower (yellow, 2), Higher (red, 12); (**B**,**D**) Upregulated (green, -2), Downregulated (red, 2).

An average of 25 DE gene transcripts corresponded to the PP pathway, an average of 83 to LB, 32 to JA, and an average of 73 to SS were observed when comparisons of HiFig vs LoFig, HiFig vs NoFig, and LoFig vs NoFig were visualized using MAPMAN. Visualization of the PP (Figure 8), the LB (Figure 9), the JA (Figure 10), and the SS (Figure 11) pathways were indicative of where the numerous DE genes were located. All DE genes presented in this work were summarized and placed into a table (Table 5). Heatmaps were recorded and compared to the NCBI databases for further gene identification (Table S1) and MAPMAN pathway genes that indicated differential expression were identified and presented (Table S2).

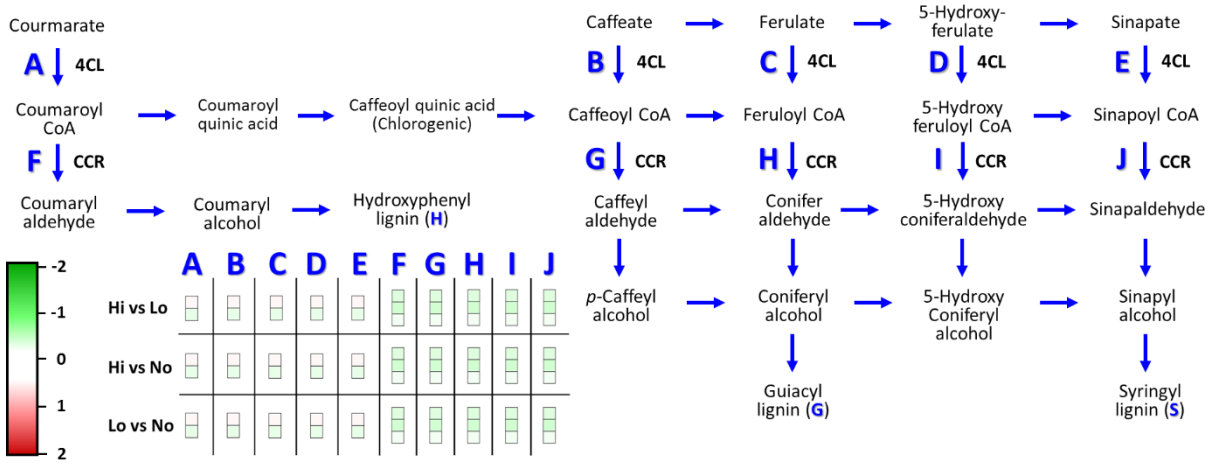

Figure 8: Depiction of Phenylpropanoid Pathway gene expression using MapMan. Upregulated (green, -2). Downregulated (red, 2).

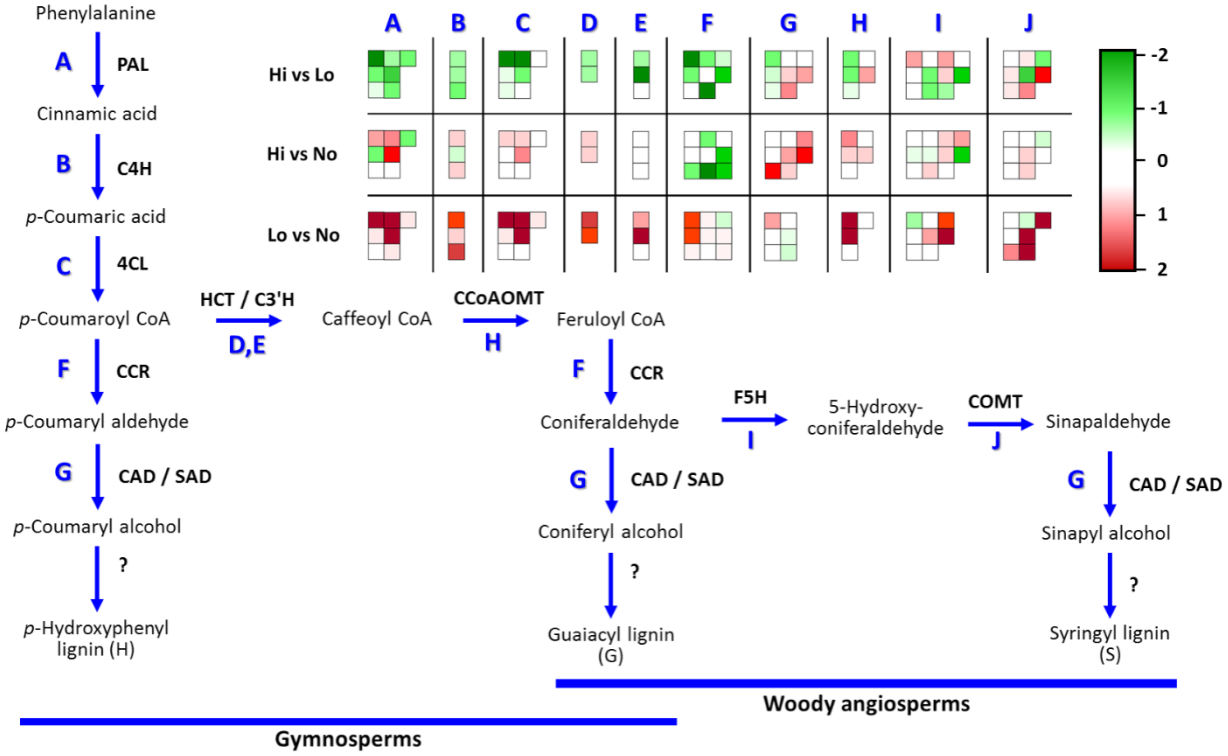

Figure 9: Depiction of Lignin Biosynthesis Pathway gene expression using MapMan. Upregulated (green, -2). Downregulated (red, 2).

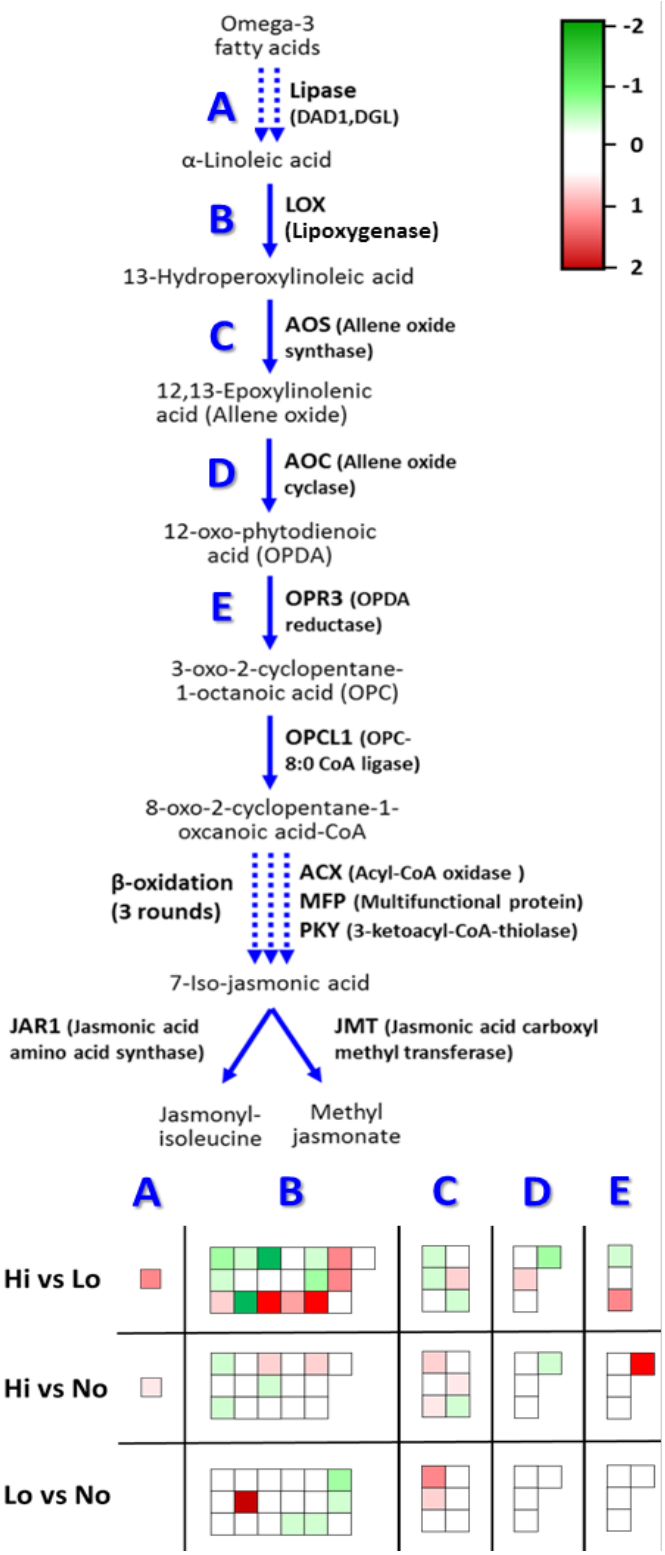

Figure 10: Depiction of Jasmonate Biosynthesis Pathway gene expression using MapMan. Upregulated (green, -2). Downregulated (red, 2).

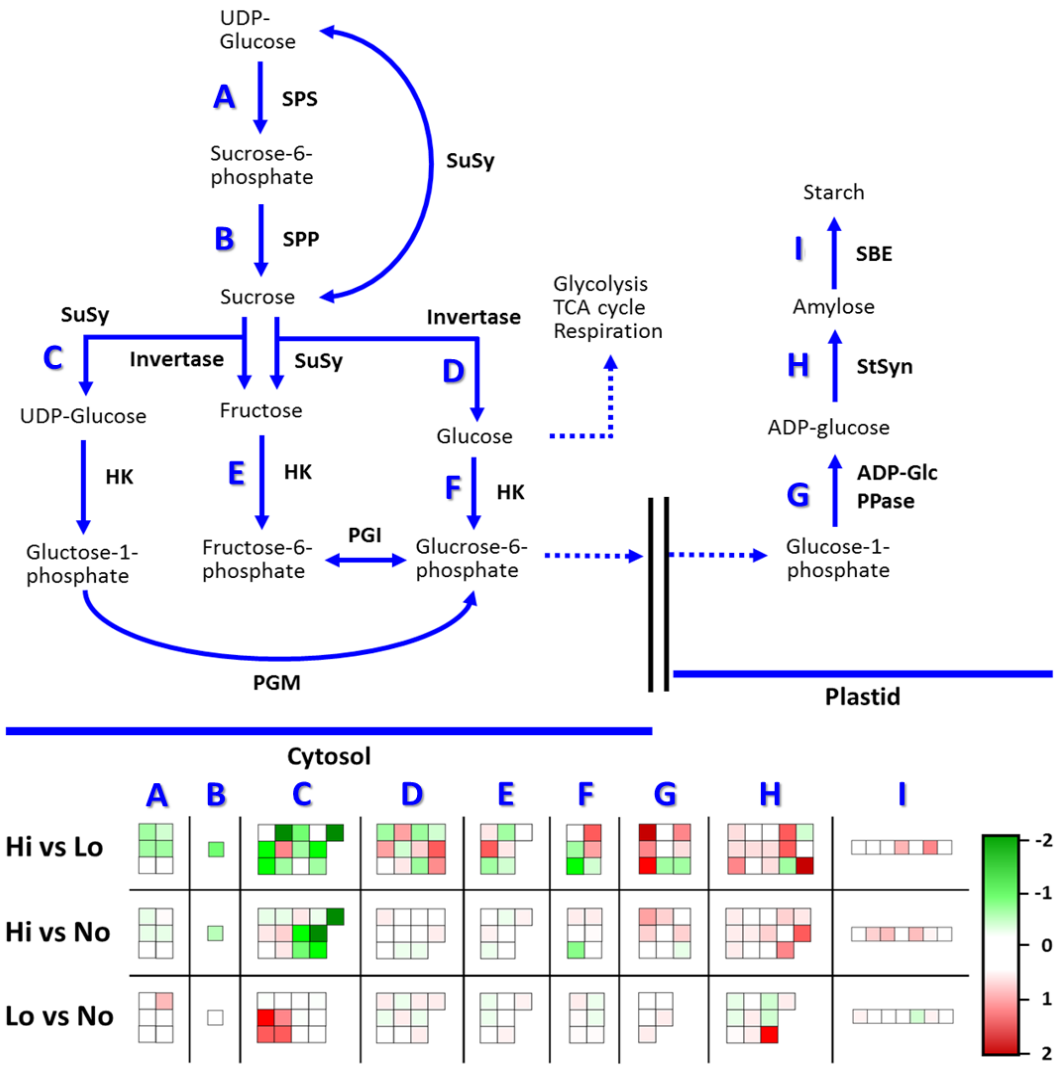

Figure 11: Depiction of Sucrose-Starch Biosynthesis Pathway gene expression using MapMan. Upregulated (green, -2). Downregulated (red, 2).

Discussion

There exists within this data a surfeit amount of evidence suggesting a genetic basis for figure however lack of available genotyping data for the harvested trees negates our ability to rule out any familial interactions. Nevertheless, these results represent the first comprehensive analysis of the presence or absence of figure in koa and the first transcriptomic-based analysis for figure in any tree species. Although results from this study do not exclude the possibility of additional environmental interactions, application of this cutting-edge approach to solve an age-old problem represents the first step towards eliminating the mystery of figure formation.

For numerous genes differentially expressed in the HiFig to Lo- and NoFig samples (Pattern 4) however, some of the most distinct ones were only captured using the in-depth pathway analysis conducted. As the examination of the nearly nine thousand genes that displayed Pattern 4 was beyond the scope of this study, only a subset of those genes relevant to Pattern 2 (HiFig and LoFig to NoFig) or a selection of biosynthesis pathways involved in wood formation were further studied.

Examination of Pattern 2 DE genes indicated that the WAT1 (Walls Are Thin1) gene and the 5NG4 gene are both significantly upregulated in figured individuals. The WAT1 gene is implicated in secondary cell wall formation and wood fiber thickness and is also involved in auxin transport and homeostasis [22,23]. Several isoforms of this gene were observed to be significantly DE and all

showed the same pattern of expression when compared to NoFig individuals. Expression of the 5NG4 gene was significantly greater in HiFig, then LoFig, and finally NoFig individuals. As with WAT1, this gene also functions in auxin biosynthesis as demonstrated by Busov et al. [24] with loblolly pine (*Pinus taeda* L.). The 5NG4 gene was shown to be highly conserved in other model species and was involved in auxin induced adventitious root formation [24]. Also, downregulation of WAT1 led to cell elongation defects and significantly decreased cell wall fiber counts [23,25]. Thus, two of the primary genes isolated within the Pattern 2 cohort also play roles in hormone biosynthesis in other species.

Many genes that stand out in terms of DE within the 4 biosynthesis pathways chosen for further study. In the PP pathway, the isoflavone reductase (IFR) family was the most represented during the analyses. These genes are produced most often in leguminous species and have numerous functions from disease resistance [26,27] and secondary metabolism [28-30] to formation of root nodules [31]. Recent reports indicated that IFR can influence biosynthesis of lignin as well [32].

Examination of the LB pathway indicated that cinnamoyl-CoA reductase (CCR), the first enzyme in the lignin biosynthesis pathway, displayed significantly lower levels of expression in HiFig individuals when compared to LoFig and NoFig. Similar to results from work done by Yong et al. [33], we found many known pathway genes to be differentially expressed between the figured groups. Worthy of note is that our data revealed several CCR gene homologs within each tree. Previous studies have shown that CCR homologs are likely responsible for the variety in CCR functional abilities [34,35]. CCR genes have diverse roles in plant growth and development [36,37] ranging from drought stress responses [34,35] to lignification [38]. Multiple studies have noted that downregulation of CCR led to decreased overall lignin content [35,39]. Here, we noted significantly decreased levels of CCR in highly figured compared to non-figured koa.

Lipoxygenases (LOXs) represent initial enzymes activated during jasmonic acid synthesis and are involved in the plant response to abiotic stress conditions [40,41]. Typically induced during wounding [41,42], these genes may also have additional functions in plants [43]. Thus, the LOX genes identified in this analysis of koa may have been induced in response to felling, the cold treatment, or may be serving additional, uncharacterized, roles in figure formation. In addition, as noted by the significant expression differences in LOX, it is possible that several of the DE abiotic stress genes responsible for cold tolerance regulation were triggered by our preservation treatments to ensure RNA stability. Differentiation between genes exhibiting abiotic stress responses and those lox genes playing a role in figure formation is difficult. However, as many other expression changes were observed in highly figured samples, there existed no shortage of supportive evidence that presence of the various expression changes was not an artifact of extraction conditions. The direct role of any one transcript in generation of figure is not yet understood however, we note WAT1 and 5NG4 as candidates for future, more directed studies of the figured wood phenomenon.

The combination of DE patterns witnessed in these specific genes along with the pathways affected leads one to believe that such expression changes may be associated with the formation of figure. At the very least, the unique patterns of expression that differentiate figured koa from non-figured koa have been identified. Use of files included in the supplemental information will allow interested parties to continue more in-depth research into additional DE pathway genes uncovered in this work that were not highlighted.

Conclusions

This study examined upregulation and downregulation of a selected subset of genes found to be significantly expressed in figured wood when compared to non-figured wood samples. Many of these genes are known to play numerous roles in plant growth and development but their functions in the formation of figured wood have yet to be identified. *De novo* assembly and RNAseq of the koa wood transcriptome were used to identify genes involved in development of figured wood. The objective of this study was to identify and examine transcripts differentially expressed to a significant level in HiFig, LoFig, and NoFig koa wood samples. Highlighted genes were then mapped to the phenylpropanoid, lignin biosynthesis, jasmonic acid biosynthesis, and sucrose – starch synthesis pathways. Numerous additional genes were differentially expressed but were not directly implicated in the pathways investigated here and thus, were not highlighted for further study at this time. These additional genes, however, may also play roles in the development of figured wood. Conversely, further investigations into the genes DE in this work but not highlighted in one of the four pathways pinpointed will likely implicate other uninvestigated pathways involved in the formation of figure in *Acacia koa*. The direct role of these transcripts in the generation of figure is not yet understood however, these data are the first to provide a starting point for future, more directed gene studies into the figured wood phenomenon.

Acknowledgements

The authors would like to thank Mr. Sagar Utturkar and Drs. Mark Coggeshall, Ratnam Wickneswari, and Melissa Wong for valuable and insightful feedback on the manuscript. We thank Drs. J.B. Friday and Faith Inman for providing the cookie samples. We acknowledge the State of Hawaii Department of Land and Natural Resources (DLNR) – Division of Forestry and Wildlife (DOFAW) and/or State Parks, as well as the USDA Forest Service (FS) as land managers and administrators for the Hawaii Experimental Tropical

Forest. This project was funded by the USDA Forest Service and The Atherton Family Foundation.

Conflict of Interest Statement

The authors declare that the research was conducted in the absence of any commercial or financial relationships that could be construed as a potential conflict of interest.

References

1. Plomion C, Leprovost G, Stokes A (2001) Wood formation in trees. Plant Physiol 127: 1513-1523.
2. Stevanic JS, Salme L (2009) Orientation of the wood polymers in the cell wall of spruce wood fibres. Holzforschung 63: 497-503.
3. Kliger IR (2001) Spiral grain on logs under bark reveals twist-prone raw material. Forest Prod J 51: 61-73.
4. Thinley C, Palmer G, Vanclay JK, Henson M (2005) Spiral and interlocking grain in *Eucalyptus dunnii*. Holz Roh Werkst 63: 372-379.
5. Denzler JK, Weidenhiller A, Golser M (2015) Property relationships between spruce logs and structural timber. Scand J Forest Res 30: 617-623.
6. Beals HO, Davis TC (1977) Figure in Wood: An Illustrated Review. Auburn, AL, Auburn University Experiment Station. Pg No: 73-77.
7. Brémaud I, Cabrolier P, Gril J, Clair B, Gérard J, et al. (2009) Identification of anisotropic vibrational properties of Padauk wood with interlocked grain. Wood Sci Technol 44: 355-367.
8. Baker PJ, Scowcroft PG, Ewel JJ (2009) Koa (*Acacia koa*) Ecology and Silviculture. General Technical Report PSW-GTR-211.
9. McKenna J, Geyer WA, Woeste KE, Cassens DL (2015) Propagating Figured Wood in Black Walnut. Open J Forest 5: 518-525.
10. Bragg DC (1999) The birdseye figured grain in sugar maple (*Acer saccharum*): literature review, nomenclature, and structural characteristics. Can J Forest Res 29: 1637-1648.
11. Bragg DC, Mroz GD, Reed DD (1997) Relationship between ''birdseye'' sugar maple (*Acer saccharum*) occurrence and its environment. Can J Forest Res 27: 1182-1191.
12. Fornale S, Rencoret J, Garcia-Calvo L, Capellades M, Encina A, et al. (2015) Cell wall modifications triggered by the down-regulation of coumarate-3-hydroxylase-1 in maize. Plant Sci 236: 272-282.
13. Ziebell A, Gjersing E, Hinchee M, Katahira R, Sykes RW, et al. (2016) Downregulation of p-coumaroyl quinate/shikimate 3-hydroxylase (C3H) or cinnamate-4-hydrolylase (C4H) in *Eucalyptus urophylla* X *Eucalyptus grandis* leads to increased extractability. Bioenergy Res 9: 691-699.
14. Sturm A, Tang G-Q (1999) The sucrose-cleaving enzymes of plants are crucial for development, growth and carbon partitioning. Trends Plant Sci 4: 401-407.
15. Thines B, Katsir L, Melotto M, Niu Y, Mandaokar A, et al. (2007) JAZ repressor proteins are targets of the SCF COI1 complex during jasmonate signalling. Nature 448: 661-666.
16. Martin D, Tholl D, Gershenzon J, Bohlmann J (2002) Methyl Jasmonate Induces Traumatic Resin Ducts, Terpenoid Resin Biosynthesis, and Terpenoid Accumulation in Developing Xylem of Norway Spruce Stems. Plant Physiol 129: 1103-1018.
17. Reinbothe C, Springer A, Samol I, Reinbothe S (2009) Plant oxylipins: role of jasmonic acid during programmed cell death, defence and leaf senescence. FEBS J 276: 4666-4681.
18. Zdyb A, Demchenko K, Heumann J, Mrosk C, Grzeganek P, et al. (2011) Jasmonate biosynthesis in legume and actinorhizal nodules. New Phytol 189: 568-579.
19. Dzialuk A, Chybicki I, Welc M, Śliwińska E, Burczyk J (2007) Presence of triploids among oak species. Ann Bot 99: 959-964.
20. Yin T, Difazio SP, Gunter LE, Zhang X, Sewell MM, et al. (2008) Genome structure and emerging evidence of an incipient sex chromosome in *Populus*. Genome Res 18: 422-430.
21. Chagné D, Kirk C, Whitworth C, Erasmuson S, Bicknell R, et al. (2015) Polyploid and aneuploid detection in apple using a single nucleotide polymorphism array. Tree Genet Genomes 11: 1-6.
22. Baba K, Karlberg A, Schmidt J, Schrader J, Hvidsten TR, et al. (2011) Activity-dormancy transition in the cambial meristem involves stage-specific modulation of auxin response in hybrid aspen. Proc Natl Acad Sci USA 108: 3418-3423.
23. Ranocha P, Dima O, Nagy R, Felten J, Corratgé-Faillie C, et al. (2013) Arabidopsis WAT1 is a vacuolar auxin transport facilitator required for auxin homoeostasis. Nat Commun 4: 2625-2633.
24. Busov VB, Johannes E, Whetten RW, Sederoff RR, Spiker SL, et al. (2004) An auxin-inducible gene from loblolly pine (*Pinus taeda* L.) is differentially expressed in mature and juvenile-phase shoots and encodes a putative transmembrane protein. Planta 218: 916-927.
25. Ranocha P, Denancé N, Vanholme R, Freydier A, Martinez Y, et al. (2010) Walls are thin 1 (WAT1), an *Arabidopsis* homolog of *Medicago truncatula* NODULIN21, is a tonoplast-localized protein required for secondary wall formation in fibers. Plant J 63: 469-483.
26. Brandalise M, Severino FE, Maluf MP, Maia IG (2009) The promoter of a gene encoding an isoflavone reductase-like protein in coffee (Coffea arabica) drives a stress-responsive expression in leaves. Plant Cell Rep 28: 1699-1708.
27. Toyoda K, Ikeda S, Morikawa JI, Hirose M, Maeda A, et al. (2013) The *Medicago truncatula-Mycosphaerella pinodes* interaction: A new pathosystem for dissecting fungal-suppressor-mediated disease susceptibility in plants. J Gen Plant Pathol 79: 1-11.
28. Shoji T, Winz R, Iwase T, Nakajima K, Yamada Y, et al. (2002) Expression patterns of two tobacco isoflavone reductase-like genes and their possible roles in secondary metabolism in tobacco. Plant Mol Biol 50: 427-440.
29. Alam I, Sharmin SA, Kim KH, Yang JK, et al. (2010) Proteome analysis of soybean roots subjected to short-term drought stress. Plant Soil 333: 491-505.
30. Hua C, Linling L, Feng X, Yan W, Honghui Y, et al. (2013) Expression patterns of an isoflavone reductase-like gene and its possible roles in secondary metabolism in *Ginkgo biloba*. Plant Cell Rep 32: 637-650.
31. Rípodas C, Via VD, Aguilar OM, Zanetti ME, Blanco FA (2013) Knockdown of a member of the isoflavone reductase gene family impairs plant growth and nodulation in *Phaseolus vulgaris*. Plant Physiol Biochem 68: 81-89.
32. Qian X, Xu S-Z, Zhao C-L, Meng H-L, Wen G-S (2015) cDNA cloning and expression analysis of the isoflavone reductase-like gene of *Dendrobium officinale*. Pak J Bot 47: 1265-1270.

33. Yong SYC, Choong CY, JA, Mat-Isa MN, Hedley P, Milne L, et al. (2011) Analysis of ESTs generated from inner bark tissue of an *Acacia auriculiformis* x *Acacia mangium* hybrid. Tree Genet Genomes 7: 143-152.

34. Lauvergeat V, Lacomme C, Lacombe E, Lasserre E, Roby D, et al. (2001) Two cinnamoyl-CoA reductase (CCR) genes from Arabidopsis thaliana are differentially expressed during development and in response to infection with pathogenic bacteria. Phytochemistry 57: 1187-1195.

35. Li J, Fan F, Wang L, Zhan Q, Wu P, et al. (2016) Cloning and expression analysis of cinnamoyl-CoA reductase (CCR) genes in sorghum. Peer J 4: e2005.

36. Boudet AM (2001) Lignins and lignification: Selected issues. Plant Physiol Bioch 38: 81-96.

37. Barakat A, Yassin NBM, Park JS, Choi A, Herr J, et al. (2011) Comparative and phylogenomic analyses of cinnamoyl-CoA reductase and cinnamoyl-CoA-reductase-like gene family in land plants. Plant Sci 181: 249-257.

38. Xue J, Luo D, Xu D, Zeng M, Cui X, et al. (2015) CCR1, an enzyme required for lignin biosynthesis in Arabidopsis, mediates cell proliferation exit for leaf development. The Plant J 83: 375-387.

39. Chabannes M, Barakat A, Lapierre C, Marita JM, Ralph J, et al. (2001) Strong decrease in lignin content without significant alteration of plant development is induced by simultaneous down-regulation of cinnamoyl CoA reductase (CCR) and cinnamyl alcohol dehydrogenase (CAD) in tobacco plants. Plant J 28: 257-270.

40. Hou Y, Meng K, Han Y, Ban Q, Wang B, et al. (2015) The persimmon 9-lipoxygenase gene *D*kLOX3 plays positive roles in both promoting senescence and enhancing tolerance to abiotic stress. Front Plant Sci 6: 1073-1088.

41. Bae KS, Rahimi S, Kim YJ, Devi BSR, et al. (2015) Molecular characterization of lipoxygenase genes and their expression analysis against biotic and abiotic stresses in *Panax ginseng*. Eur J Plant Pathol. 145: 331-343.

42. Turner J, Ellis C, Devoto A (2002) The jasmonate signal pathway. Plant Cell 14: S153-S164.

43. Pierron RJG, Pouzoulet J, Couderc C, Judic E, Compant S, et al. (2016) Variations in Early Response of Grapevine Wood Depending on Wound and Inoculation Combinations with *Phaeoacremonium aleophilum* and *Phaeomoniella chlamydospora*. Front Plant Sci 7: 1-14.